Accepted Manuscript

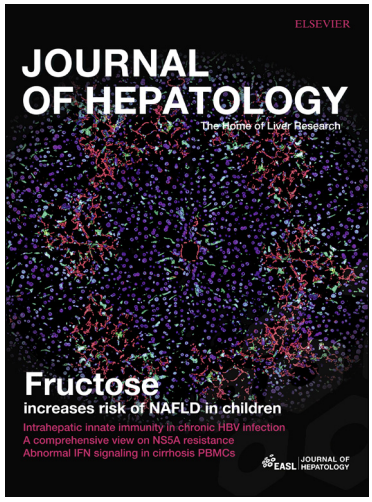

Histological Subtypes of Hepatocellular Carcinoma Are Related To Gene Mutations and Molecular Tumour Classification

Julien Calderaro, Gabrielle Couchy, Sandrine Imbeaud, Giuliana Amaddeo, Eric Letouzé, Jean-Frédéric Blanc, Christophe Laurent, Yacine Hajji, Daniel Azoulay, Paulette Bioulac-Sage, Jean-Charles Nault, Jessica Zucman-Rossi

PII: S0168-8278(17)32050-0
DOI: http://dx.doi.org/10.1016/j.jhep.2017.05.014
Reference: JHEPAT 6539

To appear in: *Journal of Hepatology*

Received Date: 10 February 2017
Revised Date: 10 April 2017
Accepted Date: 15 May 2017

Please cite this article as: Calderaro, J., Couchy, G., Imbeaud, S., Amaddeo, G., Letouzé, E., Blanc, J-F., Laurent, C., Hajji, Y., Azoulay, D., Bioulac-Sage, P., Nault, J-C., Zucman-Rossi, J., Histological Subtypes of Hepatocellular Carcinoma Are Related To Gene Mutations and Molecular Tumour Classification, *Journal of Hepatology* (2017), doi: http://dx.doi.org/10.1016/j.jhep.2017.05.014

Histological Subtypes of Hepatocellular Carcinoma Are Related To Gene Mutations and Molecular Tumour Classification

Short title: Phenotypic and molecular correlations in HCC

Julien Calderaro[1,2,3], Gabrielle Couchy[1], Sandrine Imbeaud[1], Giuliana Amaddeo[3,4,5], Eric Letouzé[1], Jean-Frédéric Blanc[6,7], Christophe Laurent[8], Yacine Hajji[1], Daniel Azoulay[3,9], Paulette Bioulac-Sage[7,10], Jean-Charles Nault[1,11], Jessica Zucman-Rossi[1,12].

1. Inserm, UMR-1162, Functional Genomics of Solid Tumors, Equipe Labellisée Ligue Contre le Cancer, Université Paris Descartes, Université Paris Diderot, Université Paris 13, France. F-75010 France.

2. Assistance Publique–Hôpitaux de Paris, Department of Pathology, CHU Henri Mondor, Créteil, France.

3. Université Paris Est Créteil, Faculté de Médecine, Créteil, France.

4. Assistance Publique–Hôpitaux de Paris, Department of Hepatology, CHU Henri Mondor, Créteil, France.

5. Inserm U955, Team 18, Créteil, France.

6. Department of Hepatogastroenterology and digestive oncology, CHU Bordeaux, Hôpital Haut-Lévêque, 33600, Pessac.

7. Inserm UMR 1053, Université de Bordeaux, 33076 Bordeaux France.

8. Department of Digestive and Endocrine Surgery, CHU-Hôpitaux de Bordeaux, France.

9. Department of Digestive and Hepatobiliary Surgery, Assistance Publique-Hôpitaux de Paris, Centre Hospitalier Universitaire Henri Mondor, 94000 Créteil, France.

10. Department of Pathology, Pellegrin Hospital, CHU Bordeaux, Bordeaux 33076, France.

11. Liver unit, Hôpital Jean Verdier, Hôpitaux Universitaires Paris-Seine-Saint-Denis, Assistance-Publique Hôpitaux de Paris, Bondy, France.

12. Assistance Publique–Hôpitaux de Paris, Department of Oncology, Hopital Européen Georges Pompidou, Paris, France.

Keywords: Histopathology, Hepatocellular carcinoma, Mutations, Molecular carcinogenesis.

Correspondence:
Jessica Zucman-Rossi; MD, PhD
INSERM U 1162, Génomique fonctionnelle des tumeurs solides
27 Rue Juliette Dodu
75010 Paris, France
TEL: +33 1 53 72 51 66
FAX: +33 1 53 72 51 92
Email: jessica.zucman-rossi@inserm.fr

Abbreviations: AFP : alpha-foeto protein, ALB : albumin, ANGPT2 : angiopoietin 2, APOB : apolipoprotein B, ARID1A : AT-Rich Interaction Domain 1A, ARID2: AT-Rich Interaction Domain 2, ATM: ATM Serine/Threonine Kinase, BCLC: Barcelona clinic of liver cancer, CI: confidence interval, CK19 : cytokeratin 19, CRP : c-reactive protein, CTNNB1 : cadherin-associated protein beta 1, EpCAM : epithelial cell adhesion molecule, GS : glutamine synthetase HBV : hepatitis B virus, HCC : hepatocellular carcinoma, HCV, : hepatitis C virus, IL6 : interleukin-6, JAK : Janus Kinase, NFE2L2: nuclear factor, erythroid 2 Like 2, OR: odds ratio, PCR: polymerase chain reaction, RPS6KA3: Ribosomal Protein S6 Kinase A3, STAT: signal transducer and activator of transcription, TERT : telomerase reverse transcriptase, TP53 : tumour protein 53, TSC1 : tuberous sclerosis 1, TSC2: tuberous sclerosis 2, WHO : World Health Organization.

Authors contributions:
Study design: JC, JZR
Generation of experimental data: JC, GC, JCN
Analysis and interpretation of data: JC, GC, SI, YH, JCN, JZR
Collection of samples and histological and clinical data: JC, GA, DA, CL, JFB, PBS, JZR
Drafting of the manuscript: JC, JCN, JZR
Revision of the manuscript and approval of its final version: JC, GC, SI, GA, JFB, CL, YH, DA, PBS, JCN, JZR
Obtained funding: JZR

Financial supports: Institut National du Cancer (INCa) with the ICGC project, the MUTHEC project (PRTK14, INCa), the LABEX OncoImmunology funded by Investissement d'Avenir ANR, the Ligue Nationale Contre le Cancer (équipe labellisée) and the Fondation Bettencourt Schuller (Coup d'Elan), Award Raymond Rosen 2016 (FRM).

Conflict of interests: the authors have no conflicts of interests related to the manuscript.

Word count: 4263.

Abstract

Background and aims: Our increasing understanding of hepatocellular carcinoma (HCC) biology holds promise for personalized care, however its translation into clinical practice requires a precise knowledge of its relationship to tumour phenotype.
Methods: We aimed at investigating molecular-phenotypic correlations in a large series of HCC. To this purpose, 343 surgically resected HCC were investigated by pathological review, immunohistochemistry, gene expression profiling and sequencing.
Results: *CTNNB1* (40%) and *TP53* (21%) mutations were mutually exclusive and defined two major groups of HCC characterized by distinct phenotypes. *CTNNB1* mutated-tumours were large (P=0.002), well-differentiated (P<0.001), cholestastic (P<0.001), with microtrabecular (P<0.001) and pseudoglandular (P<0.001) patterns and without inflammatory infiltrates (P<0.001). *TP53* mutated-tumours were poorly-differentiated (P<0.001) with compact pattern (P=0.02), multinucleated (P=0.01) and pleomorphic (P=0.02) cells and frequent vascular invasion (P=0.02). World Health Organization (WHO) histological subtypes were also strongly related to molecular features. The scirrhous subtype was associated with *TSC1/TSC2* mutations (P=0.005), epithelial-to-mesenchymal transition and a progenitor expression profile. The steatohepatitic subtype showed frequent IL-6/JAK/STAT activation without *CTNNB1*, *TERT* and *TP53* pathway alterations (P=0.01). Pathological review identified a novel subtype, designated as "macrotrabecular-massive" associated with poor survival (P<0.001), high alphafoeto-protein serum level (P=0.02), vascular invasion (P<0.001), *TP53* mutations (P<0.001) and *FGF19* amplifications (P=0.02), features also validated in TCGA data. Finally, integration of HCC pathological characteristics with its transcriptomic classification showed phenotypically distinct tumour subclasses closely related to G1-G6 subgroups.
Conclusion: HCC phenotypes are tightly associated with gene mutations and transcriptomic classification. These findings may help in translating our knowledge of HCC biology into clinical practice.

LAY SUMMARY: HCC is a very heterogenous tumor, both at the pathological and molecular levels. We show here that HCC phenotype is tightly associated to its molecular alterations and underlying oncogenic pathways.

Introduction

Malignant primary liver tumours are the second leading cause of cancer-related death worldwide, with an increasing incidence in almost all countries [1]. They are mainly represented by hepatocellular carcinoma (HCC) that results from the malignant transformation of hepatocytes. The most frequent risk factors of HCC comprise alcohol intake, infection by hepatitis B (HBV) or hepatitis C (HCV) viruses, and metabolic syndrome [2]. Although surveillance protocols of patients at-risk to develop HCC have significantly improved, clinical outcome remains poor with a majority of patients presenting with advanced disease not eligible for curative therapy [3].

At the pathological level, HCC is a morphologically heterogeneous tumour [4, 5]. If HCC neoplastic cells most often grow in cords of variable thickness lined by endothelial cells mimicking the trabeculae and sinusoids of normal liver, other architectural pattern are frequently observed and numerous cytological variants are also recognized, comprising clear, pleomorphic, or bile producing cells [4-6]. Moreover, several HCC subtypes defined by distinctive and easily recognizable histological features have been identified [4, 5, 7]. In the last decade, there has been a growing interest for a particular subtype of HCC with so-called "progenitor features". Thought to derive from progenitor cells, this tumour subtype shares an overlapping gene expression profile with oval cells and fetal hepatoblasts [8]. It is characterized by an adverse clinical outcome and immunohistochemical expression of cytokeratin 19 (CK19) by more than 5% of neoplastic cells is usually considered as a surrogate marker of this variant [9].

In parallel to this pathological heterogeneity, gene expression profiling has allowed the establishment of several HCC transcriptomic classifications [10-14]. Our group proposed a classification comprising 6 subclasses associated with clinical and genetic features [11]. Groups G1 to G3 are characterized by chromosomal instability, cell cycle activation, *TP53* mutations (G2-G3) and HBV infection (G1-G2), while groups G4 to G6 are associated with chromosomal stability and Wnt/β-catenin pathway activation mainly due to activating *CTNNB1* mutations (G5-G6) [11].

High-throughput sequencing techniques have also defined the comprehensive mutational landscape of HCC. The most frequent mutations and chromosome alterations were identified in *TERT* promoter, *CTNNB1, TP53, AXIN1, ARID1A, NFE2L2, ARID2* and *RPS6KA3* [15-20].

Although this increasing understanding of HCC biology holds promise for future targeted therapies and personalized care, its translation into clinical practice will require a precise knowledge of its relationship to tumour phenotype. Here, we aimed to determine how HCC molecular features relate to its phenotype by combining comprehensive pathological analyses, gene expression profiling and gene sequencing in a series of 343 resected tumours developed in patients with various underlying liver diseases.

Material and methods

Patients and samples

A total of 343 unselected HCC developed in 339 patients treated by surgical resection in 2 French university hospitals (Henri Mondor, Créteil and Pellegrin, Bordeaux) were included in the study ("InsermU1162 Cohort") (the overall study design and flow chart is provided in the supplemental material and methods). Tumour and non-tumour liver samples were frozen immediately after surgery and stored at -80°C. All patients were treatment naïve before surgery and informed consent was obtained in all cases. The study was approved by institutional review board committees (CCPRB Paris Saint Louis, 1997, 2004, 2010 and 2016, approval number 2016/57NICB; Bordeaux 2010-A00498-31).
The following clinical and biological features were systematically recorded: age (recoded as >60 or ≤60 years), gender, liver disease etiology (infection by HBV or HCV, alcohol intake, metabolic syndrome, hereditary hemochromatosis or undetermined), Barcelona Clinic of Liver Cancer (BCLC) stage, pre-operative alpha-foeto protein (AFP) serum levels (recoded as >100ng/ml or ≤100ng/ml) and follow-up (early relapse and disease-specific survival).

Pathological examination

For each case, all available histological slides were reviewed by 2 expert pathologists (JC and PBS) specialized in liver disease and blinded to the clinical and molecular characteristics. A training set of 60 tumours was first used to determine the reviewing and quotation method (Supplemental Table 1), then all features were recorded by the two pathologists during common review sessions. Cases with disagreement were discussed and a consensus was reached.

The following histological features were systematically assessed: tumour differentiation (according to Edmondson-Steiner grade), satellite nodules, macrovascular or microvascular invasion, tumour capsule, microtrabecular, macrotrabecular, pseudoglandular or compact pattern, pleomorphic cells, cholestasis, multinucleated cells, clear cells, sarcomatous changes, hyaline bodies, inflammatory infiltrates, steatohepatitic, scirrhous, lymphoepithelioma-like, and sarcomatoid subtypes (Supplemental Table 1) [5, 7, 21, 22]. To reflect the co-existence of several histological features within the same tumour, architectural patterns and cytological variants identified in at least 20% of the tumour were considered present (Supplemental Table 1).
During the review of the training set of tumors, we observed cases with a striking predominant macrotrabecular architecture involving more than 50% of the tumor. Their microscopic appearance indeed mainly consisted of neoplastic cells arranged in thick trabeculae coated by endothelial cells and surrounded by dilated vascular spaces. Trabeculae observed in cross sections also appeared as endothelium-coated tumor clusters. A link between the macrotrabecular architecture and poor clinical outcome has been previously suggested [23], and we further aimed to assess if those cases may constitute a novel HCC subtype. This novel candidate subtype was further designated as “macrotrabecular-massive HCC” (MTM-HCC).
Validation of the relevance of this subtype was further performed using the public database from The Cancer Genome Atlas (TCGA) Research Network, which consists in a

large series of HCC samples with available clinical annotations, digital slides, and molecular data. [24, 25] The website (www.cbioportal.org) was accessed on December 2016. One digital slide was available for each case, and, after the exclusion of cases with histological features suggestive of either cholangiocarcinoma (n=8) or hepatocholangiocarcinoma (n=3), a series of 359 HCC with molecular data was finally selected for further analysis ("TCGA Cohort"). For survival and early relapse studies, patients with a prior history of anti-tumour treatment and/or incomplete surgical resection (R1 or R2) were excluded. Survival and relapse status were available in 313 and 277 cases, respectively.

Immunohistochemistry

Expression of Glutamine Synthetase (GS), β-catenin, CK19, Epithelial cell adhesion molecule (EpCAM), C-reactive protein (CRP), ARID1A, phospho-S6 protein, and phospho-ERK was investigated on whole tumour sections to avoid sampling heterogeneity inherent to tissue-micro-array techniques. Stainings were performed manually or using Leica Bondmax or Dako autostainers (a detailed description of quotation methods, antibodies used and staining protocols is provided in Supplemental Table 1, Supplemental Material and Methods and CTAT table).

Transcriptomic classification of HCC samples and gene expression

Total RNAs were extracted with the RNeasy kit (Qiagen®), and quality assessment was performed as previously described.[26] Five hundred nanograms of RNA were further reverse-transcribed using the High Capacity Transcription kit (Life technologies®). After preamplification of the specific targets, Real-Time Polymerase Chain Reaction (PCR) was performed using the high throughput BioMark Real-Time PCR system (Fluidigm®, South San Francisco, CA) according to manufacturer's instructions, using Fluidigm 96.96 dynamic arrays and TaqMan predesigned assays (Supplemental Material and Methods). Ct values were calculated using the Fluidigm Real-Time PCR Analysis software (4.1.3). Gene expression was normalized to ribosomal 18S mRNA, and expression level of the tumour samples was compared with the mean level of the corresponding gene expression in normal liver tissues (n = 5), expressed as an n-fold ratio. The relative amount of RNA was calculated with the 2-delta delta CT method.

Transcriptomic classification of HCC samples was performed in 265 cases using a combination of 16 genes, as previously described.[11] In addition, the expression of the following genes was investigated in a subset of 186 tumours: *ALB, AFP, APOB, CYP1A1, CYP1A2, CYP3A4, CYP2E1, CYP2C9, HNF4A, HNF1A* (hepatocellular differentiation and function), *GCK, GCKR, GPI* (glycolysis), *FBP1, PCK1, PCK2* (gluconeogenesis), *ACACA, ACLY, FADS1, FADS2, FASN, ME1* (fatty acid synthesis), *ABCB11, ABCG2, ABCB4, ABCC2, ABCB1, SLC01B3* (transporters involved in bile salts efflux into canaliculi), *ABCC1*, *ABCC3*, *ABCC4* (transporters involved in bile salts efflux into blood flow), *GLUL, LGR5, TBX3* (Wnt/β-catenin pathway target gene), *MKI67, RRM2, AURKA, EZH2* (cell proliferation), *ANGPT1*, *ANGPT2, VEGFA* (angiogenesis), *KRT19, EPCAM, SOX9, SALL4*, *ALDH1A, CD44, CD24, KRT7, CD133, THY1* (progenitor/cancer stem cell markers), and *TGFB1, TGFβR1, SMAD4 and VIM* (TGFβ pathway/epithelial-to-mesenchymal transition) (Supplemental Material and Methods).

Gene sequencing

For 129 cases, we extracted data from our former whole-exome sequencing study and selected genes mutated or altered in at least 5% of the tumours (*TERT* promoter, *CTNNB1* exon 3, *TP53, ALB, ARID1A, AXIN1, APOB, NEF2L2, ARID2, TSC1/TSC2, ATM, CDKN2A, ACVR2A, RPS6KA3, FGF19*) [16]. For additional cases, genomic DNA was extracted using a Promega Maxwell® Instrument and samples were further sequenced for *TERT* promoter, *CTNNB1*, *TP53*, *AXIN1*, *ALB*, *APOB*, *ARID1A, ARID*2, *NFE2L2*, *ATM*, *TSC1/TSC2* and *RPS6KA3*, using a MiSeq instrument (Illumina, San Diego, CA, USA) (Supplemental Material and Methods), or direct Sanger sequencing, as previously described [15]. It has been formerly demonstrated that HCC display a relatively modest degree of intra-tumour heterogeneity regarding driver genetic alterations [27-29], and one frozen sample was available and analyzed for each case.

Statistical analysis

Statistical analysis was performed using R software (3.2.2). Comparison between qualitative and quantitative data was performed using Chi-square and Fisher exact tests and Mann-Whitney U and Kruskall-Wallis tests, respectively. Monte-Carlo method was used to adjust the P value for multiple tests. Patients with curative (R0) resection (n=278) and features with more than 10% infrequency were included in survival analysis. Variables associated with disease-specific survival were identified using univariate and multivariate Cox proportional hazards regression models (Wald test), using the *survival*, *rms* and *Publish* packages. Prior to the multivariate analysis, collinear variables (BCLC B-C and macrovascular invasion; macrotrabecular histological pattern and macrotrabecular-massive subtype) were first tested in a bivariate analysis and the variable with the highest OR was further included in the multivariate analysis. Kaplan-Meier plots were used to describe survival rates among all cases. All reported P values were two-tailed and differences were considered significant when the P value was under 0.05.

Results

Patients and pathological examination

The clinical features of our series were common for western patients with HCC treated by liver resection (Table 1). There was a strong male predominance (85%), with main risk factors being alcohol intake (41%), followed by HCV infection (18%) and HBV infection (17%). Mixed etiologies were observed in 15% of the patients. Different disease stages were included with very early/early (BCLC 0-A, 67%) as well as intermediate/advanced (BCLC B-C, 33%) tumours. High AFP protein levels (>100ng/ml) were detected in 28% of the patients. As expected in a series of surgically resected HCC, we identified a high rate of non-cirrhotic patients (F0-F1 38%, F2-F3 33%, F4 29%). Early relapse and disease-related death occurred in 41% (115/278) and 33% (92/278) of the patients, respectively.

Tumours were frequently large (61% with diameter >50mm), with satellite nodules (46%), macrovascular (18%) or microvascular (60%) invasion (Table 1). A complete fibrous capsule surrounding the tumour was identified in 11% of the cases. We observed a slight predominance of poorly differentiated HCC (Edmondson grade III-IV, 57%). A high intra-tumour heterogeneity was observed, with a median of 4 architectural patterns/cytological variants co-existing within the same tumour. Areas with microtrabecular, macrotrabecular, pseudoglandular and compact histological architectural patterns were identified in 73%, 52%, 53% and 45% of the tumours, respectively (Table 1). Among the cytological variants, we observed foci of clear cells and cholestasis in 31% and 25% of the cases, respectively. Sarcomatous changes, multinucleated cells and hyaline bodies were observed in 10-25% (Table 1). Being identified in 6% of the tumours, pleomorphic cells were the less frequent cytological variant.
Following the WHO Classification of Tumours definitions, several HCC subtypes were identified: scirrhous (5%), steatohepatitic (6%), and lymphoepithelioma-like (2%) (Table 1). No sarcomatoid HCC was observed. The novel macrotrabecular-massive subtype candidate represented 10% of the tumours.

Molecular features

Transcriptomic subgroups were determined using qRT-PCR and the 16-gene signature previously described.[11] Tumours were assigned to proliferative (G1 5%, G2 6%, G3 20%) or less proliferative (G4 34%, G5 23%, G6 12%) HCC subclasses (Table 1). We next searched for alterations of major oncogenes/tumour suppressor genes and identified mutations in *TERT* promoter (65%, n=208/322), *CTNNB1* (40%, n=130/332), *TP53* (21%, n=72/341), *ALB* (16%, n=27/170) *ARID1A* (14%, n=45/313), *AXIN1* (11%, n=34/322), *APOB* (11%, n=18/171), *ARID2* (7%, n=23/313), *NFE2L2* (6%, n=19/308), *TSC1/TSC2* (6%, 15/239), *ATM* (6%, 15/238), *RPS6KA3* (5%, n=16/311) and *ACVR2A* (5%, n=6/129) (Table 1 and Supplemental Table n°2). In addition, whole-exome sequencing analysis revealed *CDKN2A* homozygous deletions or mutations (5%, n=7/129) and *FGF19* amplifications (5%, n=6/129).

Associations between molecular alterations and HCC phenotype

CTNNB1 mutations define a specific cholestatic well-differentiated subtype of HCC. We further searched for correlations between gene mutations/alterations and pathological features. Interestingly, the major correlations were identified with *CTNNB1* exon 3 and *TP53* mutations, which showed, as formerly reported, a significant tendency towards mutual exclusivity (P<0.001) (Supplemental Table 3).[30] *CTNNB1* mutated tumours represented 40% of the series and were more frequently large (Odds ratio (OR) 2.14, P=0.002), well-differentiated (OR 2.46, P<0.001), with intact tumour capsule (OR 2.54, P=0.02), areas of microtrabecular (OR 4.32, P<0.001) and pseudoglandular (OR 3.27, P<0.001) histological patterns, tumour cholestasis (OR 6.53, P<0.001), and a lack of inflammatory infiltrates (OR 3.41, P<0.001) (Table 2 and Figure 1A-C). There were no associations of *CTNNB1* mutations with the degree of intra-tumor heterogeneity (median number of architectural patterns/cytological variants per tumor: *CTNNB1* mutated 4 vs *CTNNB1* non mutated 4). As expected, elevated mRNA levels of Wnt/β-catenin pathway targets and surrogate immunohistochemical markers of its activation (β-catenin nuclear staining and high GS expression) were also associated with *CTNNB1* mutations (P<0.001) (Supplemental Table 3 and Figure 1A, 1D and 1E). Consistent with the observed lack of inflammatory infiltrates in *CTNNB1* mutated HCC, these tumours also exhibited downregulation of the IL6/JAK/STAT pathway, with low *IL6*, *CRP* and *SAA2* mRNA levels and low CRP immunohistochemical expression (P<0.001) (Figure 1A et 1E). Lack of ARID1A immunohistochemical expression was also frequently observed (Figure 1A).

Gene expression experiments showed that *CTNNB1* mutations were associated with the maintenance of various markers of hepatocellular differentiation and function (*APOB, CYP1A1, CYP1A2, CYP3A4, CYP2E1, CYP2C9, HNF1A, HNF4A*), low *AFP* expression and low cell proliferation compared to non-mutated HCC (Figure 1E). Interestingly, a major deregulation in bile salts transporters expression (up-regulation of transporters involved in canalicular bile salts efflux and down-regulation of those responsible for bile salts efflux into blood flow) was observed and may contribute to the cholestatic phenotype of these tumours (Figure 1E and 1F).

TP53 mutated HCC are poorly differentiated, highly proliferative and macrotrabecular-massive. *TP53* mutations, identified in 21% of the tumours, were associated with poor differentiation (OR 6.41, P<0.001), macrovascular (OR 2.57, P=0.004) and microvascular (OR 2.03, P=0.02) invasion, areas of compact histological pattern (OR 1.90, P=0.02), foci of sarcomatous changes (OR 2.67, P=0.01), pleomorphic (OR 3.33, P=0.02) and multinucleated (OR 2.27, P=0.01) cells, and lack of tumour cholestasis (OR 5.75, P<0.001) (Supplemental Table 3 and Figure 2A-C). No relationship between *TP53* mutations and the degree of intra-tumor heterogeneity was observed (median number of architectural patterns/cytological variants per tumor: *TP53* mutated 4 vs *TP53* non-mutated 4). Interestingly, *TP53* mutated tumours exhibited PI3K/AKT pathway activation, as assessed by an over-expression of phospho-S6 protein by tumour cells using immunohistochemistry (Supplemental Table 3 and Figure 2A). Gene expression experiments showed an association of *TP53* mutations with increased cell proliferation, epithelial-to-mesenchymal transition and angiogenesis activation (Figure 2D).

A heat-map graphical representation of the main pathological and immunohistochemical features linked to *CTNNB1* mutated (tumour cholestasis, β-catenin nuclear staining and

high GS expression), *TP53* mutated (compact pattern, macrotrabecular-massive subtype, Edmondson-Steiner III-IV and microvascular invasion) and non-mutated (inflammatory infiltrates and CRP expression) HCC cases is provided in Figure 2E.

Noticeably, TP53 mutations were also strongly correlated to the novel macrotrabecular-massive subtype of HCC (MTM-HCC) identified during the pathological review (P<0.001) (Figure 2A and 3A-D). This subtype, representing 10% of all tumours and characterised by a predominant (>50%) macrotrabecular growth pattern, was more frequent in HBV infected patients (P=0.007), with high AFP serum levels (P=0.02) and histological features of aggressiveness (satellite nodules P<0.001, macrovascular P<0.001 and microvascular P<0.001 invasion) (Figure 3E and supplemental Table 4). Regarding molecular alterations and gene expression, we observed an association of MTM-HCC with G3 subgroup (P<0.001), *TP53* (P<0.001) and *ATM* mutations (P=0.03), *FGF19* amplifications (P=0.02), and angiogenesis activation (upregulation of ANGPT2 P=0.004 and an almost significant trend towards VEGFA overexpression P=0.07) (Figure 3E and Supplemental Table 5). This subtype also frequently demonstrated a progenitor phenotype (CK19 immunohistochemical expression P=0.02) (Figure 3E). Finally, MTM-HCC was significantly associated, in multivariate analysis, with early tumour relapse (p=0.05) and poor overall survival (p=0.03) (Table 2 and Figure 3F). Moreover, it retained a prognostic value even when patients were stratified according to the existence of microvascular invasion and satellite nodules (p<0.001).

We took advantage of the TCGA public database to validate the relevance of this novel subtype. Available digital slides were reviewed without knowledge of clinical, biological and molecular features. We identified 61 tumours (17%, 61/358) with histological features of MTM-HCC (Supplemental Table 6). We were able to validate the associations of MTM-HCC with high AFP serum levels (p=0.001), macrovascular (p=0.002) and microvascular (p=0.003) invasion, TP53 mutations (p<0.001), FGF19 amplifications (p=0.007) and activation of angiogenesis with ANGPT2 upregulation (z-scores 0.55 vs -0.18, p<0.001) (Figure 3E). MTM-HCC was also associated, in univariate analysis, with early tumour relapse (p=0.002) and poor overall survival (p=0.02) (Figure 3F).

Associations of other HCC subtypes with clinical and molecular features

We further aimed to determine the potential clinical and/or biological implications of other recognized HCC subtypes:

-The scirrhous HCC subtype, defined by marked stromal fibrosis, was characterized by *TSC1/TSC2* (P=0.005), lack of *CTNNB1* (P<0.001) mutations and CK19 expression (P<0.001) (Figure 4A-C and Supplemental Table 4). In this line, RT-PCR experiments revealed up-regulation of progenitor/cancer stem cell genes (*CD24, KRT19, THY1, CD133*), and epithelial-to-mesenchymal transition activation (*TGFβ*, *VIM*) (Figure 4D and Supplemental Table 5). A trend of increased phospho-S6 protein expression was observed (50% vs 31%, P=0.2).

-The steatohepatitic subtype of HCC was not related to specific clinical features, but displayed a less aggressive histological phenotype with a lack of satellite nodules (P=0.02) and microvascular invasion (P=0.04)(Figure 4E and F, Supplemental Table 4). At the molecular level, it was associated with the G4 transcriptomic subgroup and to a lack of Wnt/β-catenin pathway activation (lack of *CTNNB1* mutations P=0.01 and low GS expression P=0.005) (Figure 4F). Activation of the IL6/JAK/STAT pathway was frequent

with CRP immunohistochemical expression (P=0.02) (supplemental table 4 and Figure 4F). Although histological appearance of this subtype might suggest dysregulation of metabolic processes, no significant changes in genes involved in fatty acid synthesis, glycolysis or neoglucogenesis were observed (Supplemental Table 5).
-Finally, the lymphoepithelioma-like subtype was not associated with any clinical or molecular feature, however our series only comprised 6 cases of this rare variant.

Integrative analysis of the pathological phenotype with the molecular HCC classification.

For 265 tumours with available classification, we integrated the various histopathological, clinical and genetic features into to the G1-G6 transcriptomic classification to obtain a more global view of the molecular and pathological correlations. (Figure 5 and Supplemental Table 7).

Tumours belonging to the transcriptomic G1G2G3 subclasses, known to be characterized by high cell proliferation and chromosomal instability, were associated with several clinico-biological features: high AFP serum levels (G1G2G3, P<0.001), female gender (G1, P<0.001) and hemochromatosis (G3, P=0.01). Gene sequencing showed enrichment in *TP53* (G1G2G3, P<0.001), *RPS6KA3* (G1, P=0.03), *AXIN1* and *ATM* (G1G2, P=0.004 and 0.01, respectively) mutations, and *FGF19* and *TSC1/TSC2* alterations (G3, P=0.02 and 0.01, respectively). Histologically, G1G2G3 HCCs were poorly differentiated (G1G2G3, P<0.001), with frequent macrovascular invasion (G3, P=0.01) foci of clear cells (G1, P=0.001), sarcomatous changes (G1G2, P=0.02), areas of compact (G3, P=0.01) and macrotrabecular (G3, P<0.001) histological patterns, and foci of pleomorphic (G3, P=0.04) and multinucleated (G3, P<0.001) cells. The G1 subtype showed a progenitor phenotype with both CK19 (P=0.002) and EpCAM (P<0.001) immunohistochemical expression. Activation of MAPKinase and PI3K/AKT pathways, as assessed by phospho-ERK and phospho-S6 protein expression, were identified in tumours classified as G1 (P=0.02) and G3 (P=0.02), respectively (Figure 5).

Tumours classified in G4G5G6 subclasses, characterized by low cell proliferation and chromosomal stability, were most often well-differentiated (G4G5G6, P<0.001). G4 HCCs were additionally associated with small tumour size (P=0.03), lack of satellite nodules (P=0.004) and microvascular invasion (P<0.001), steatohepatitic subtype (P=0.004), inflammatory infiltrates (P=0.04) and CRP expression (P=0.01). They were also characterized by a lack of *CTNNB1* (P<0.001) and *TP53* (P=0.047) mutations (Figure 5). G5G6 subclasses, strongly associated with *CTNNB1* activating mutations (P<0.001), were related to the microtrabecular pattern of growth (P=0.01), the presence of tumour cholestasis (P<0.001) and a lack of inflammatory infiltrates (P=0.01). Immunohistochemical experiments showed Wnt/β-catenin pathway activation with β-catenin nuclear staining (P<0.001) and strong GS expression (P<0.001), along with lack of ARID1A expression (P=0.002).

Discussion

The present study revealed strong relationships linking molecular and pathological features in HCC. Two distinct HCC phenotypes were delineated by the mutually exclusive *CTNNB1* and *TP53* mutations that define 57% of all tumours. Other more infrequent molecular defects were also associated with rare pathological features such as *TSC1/TSC2* mutations and the scirrhous subtype.

CTNNB1 mutations activating ß-catenin are oncogenic driver mutations associated with a specific HCC subtype consisting in well-differentiated tumours with cholestasis and microtrabecular and pseudoglandular patterns, as previously reported [31]. Interestingly, our gene expression experiments provide additional insights into the molecular basis of the particular phenotype of *CTNNB1* mutated tumours: their good differentiation is indeed associated with the maintenance of several markers of hepatocellular differentiation and function, while the dysregulation of bile salt transporters expression may account for their cholestatic appearance. Noticeably, detection of malignant and benign *CTNNB1* mutated hepatocellular tumours by the Magnetic Resonance Imaging contrast agent gadoxetic acid has been demonstrated to rely on the overexpression of one of these transporters, *SLCO1B3*, which is responsible for bile salt uptake from the blood flow [32, 33]. In the present study, we identified an inverse correlation between intra-tumour inflammatory infiltrates and Wnt/β-catenin pathway activation. In this line, *CTNNB1* mutated HCC showed down-regulation of several components of the IL6/JAK/STAT pathway. In contrast, activation of the Wnt/β-catenin signaling pathway has been reported to induce, in the liver of modified mouse models, a specific inflammatory response with an increase of intra parenchymal inflammatory cells [34]. Discrepancies between human HCC and mouse models might indicate that ß-catenin activation could act as a pro- and anti-inflammatory signal in mice and human, respectively. Interestingly, anti-inflammatory effects were previously identified in other human tumours such as melanoma in which Wnt/β-catenin pathway activation is indeed responsible for T-cell exclusion from the intra-tumour microenvironment [35].

TP53 mutations were mostly identified in poorly differentiated tumours with frequent vascular invasion and activation of cell proliferation, angiogenesis and epithelial-to-mesenchymal transition. *TP53* inactivation was also noticeably linked to the novel macrotrabecular massive HCC subtype (MTM-HCC), the relevance of which was further confirmed by additional associations with clinical (HBV infection, early relapse and poor survival), pathological (satellite nodules and vascular invasion) and molecular (*FGF19* amplifications) features. The histological appearance of this variant, consisting of thick trabeculae surrounded by vascular spaces, was reminiscent to a particular architectural pattern first described by Sugino and collaborators in a xenograft model of a mammary tumour cell line [36]. Consisting of endothelium-coated cell clusters, this pattern was further demonstrated to promote the *in vivo* metastatic potential of a mouse HCC cell line through the release of tumour clusters into the blood stream in an epithelial-to-mesenchymal transition independent manner.[37] Silencing the expression of ANGPT2 growth factor by neoplastic cells was able to disrupt the formation of this particular pattern and reduce both intrahepatic and pulmonary metastases [37]. ANGPT2 is known to promote neoangiogenesis and endothelial sprouting in cooperation with VEGFA [38], and consistently, we observed higher *ANGPT2* mRNA levels in MTM-HCC, and an almost significant trend of increase for *VEGFA*. Our results may open novel therapeutic perspectives for this highly aggressive HCC subtype, as inhibitors of both ANGPT2 and

VEGFA signaling are available and have shown remarkable *in vivo* anti-tumour efficacy if used in combination [39].

Other well-recognized HCC subtypes were also related to clinical and/or molecular characteristics. The so-called steatohepatitic HCC is characterized by its resemblance with non-neoplastic steatohepatitis and is considered to preferentially occur in patients with metabolic syndrome [7, 21]. In our series, we did not identify any association of this subtype with liver disease etiology despite a proportion of 17% of patients with metabolic syndrome. We were however able to demonstrate, in keeping with a previous report by Ando and collaborators,[40] that steatohepatitic HCC display a particular molecular profile mainly defined by the lack of Wnt/β-catenin pathway activation. The oncogenic mechanisms involved in the progression of this variant thus remain to be identified.
A link between scirrhous HCC and progenitor traits has been previously evidenced. [41] We have here confirmed these results, with the association with CK19 expression and the upregulation of various cancer stem cell/progenitor genes, and have additionally demonstrated that this HCC subtype is also related to the activation of PI3K/AKT pathway, with *TSC1/TSC2* mutations and a trend towards phospho-S6 overexpression. Further studies will have to determine if patients with this particular variant might benefit from PI3K/AKT pathway inhibitors.

Finally, integration of clinical, genetic, and pathological features into HCC classification showed strong associations with tumour subclasses. Different oncogenic pathways drive the progression of HCC subgroups and they thus result in distinct tumour phenotypes. These findings are in keeping with those of Tan et al., who showed that clinicopathological features were associated with Hoshida HCC classification [42].

Altogether, our study provides a comprehensive overview of the relationship between HCC phenotype and its molecular characteristics. We have showed that histological features recognized by the WHO Classification of Tumours are related to particular gene mutations and transcriptomic subgroups, and further unraveled a novel histological subtype linked to molecular alterations that may have clinical relevance. Our next challenge is to validate our findings in different clinical settings, for example in advanced tumours with only biopsy samples available. However, our results already provide the tools to translate HCC molecular classification into clinical practice.

Acknowledgements

We warmly thank the TCGA Research Network, J. Saric, C. Laurent, L. Chiche, B. Le Bail and C. Castain (Centre Hospitalier Universitaire Bordeaux), D. Cherqui, A. Laurent and J. Tran Van Nhieu (Centre Hospitalier Universitaire Henri Mondor, Créteil), Tumorotheque/Plateforme des Ressources Biologiques of Bordeaux Pellegrin and Henri Mondor Hospitals, and Réseau Français des CRB foie for contributing to the tissue collection. and Servier medical art for image templates (smart.servier.fr).

References

1] Lozano R, Naghavi M, Foreman K, Lim S, Shibuya K, Aboyans V, et al. Global and regional mortality from 235 causes of death for 20 age groups in 1990 and 2010: a systematic analysis for the Global Burden of Disease Study 2010. Lancet 2012;380:2095-2128.

[2] El-Serag HB, Rudolph KL. Hepatocellular carcinoma: epidemiology and molecular carcinogenesis. Gastroenterology 2007;132:2557-2576.

[3] Forner A, Llovet JM, Bruix J. Hepatocellular carcinoma. Lancet 2012;379:1245-1255.

[4] Aaltonen LA, Hamilton SR, World Health Organization., International Agency for Research on Cancer. Pathology and genetics of tumours of the digestive system. Lyon Oxford: IARC Press ;Oxford University Press (distributor); 2000.

[5] Bosman FT, World Health Organization., International Agency for Research on Cancer. WHO classification of tumours of the digestive system, 4th ed. Lyon: International Agency for Research on Cancer; 2010.

[6] MacSween RNM, Burt AD, Portmann B, Ferrell LD. MacSween's pathology of the liver. 6th ed. Edinburgh: Churchill Livingstone,; 2011. p. 1 online resource (1 v.).

[7] Salomao M, Yu WM, Brown RS, Jr., Emond JC, Lefkowitch JH. Steatohepatitic hepatocellular carcinoma (SH-HCC): a distinctive histological variant of HCC in hepatitis C virus-related cirrhosis with associated NAFLD/NASH. The American journal of surgical pathology 2010;34:1630-1636.

[8] Lee JS, Heo J, Libbrecht L, Chu IS, Kaposi-Novak P, Calvisi DF, et al. A novel prognostic subtype of human hepatocellular carcinoma derived from hepatic progenitor cells. Nature medicine 2006;12:410-416.

[9] Durnez A, Verslype C, Nevens F, Fevery J, Aerts R, Pirenne J, et al. The clinicopathological and prognostic relevance of cytokeratin 7 and 19 expression in hepatocellular carcinoma. A possible progenitor cell origin. Histopathology 2006;49:138-151.

[10] Zucman-Rossi J, Villanueva A, Nault JC, Llovet JM. Genetic Landscape and Biomarkers of Hepatocellular Carcinoma. Gastroenterology 2015;149:1226-1239 e1224.

[11] Boyault S, Rickman DS, de Reynies A, Balabaud C, Rebouissou S, Jeannot E, et al. Transcriptome classification of HCC is related to gene alterations and to new therapeutic targets. Hepatology 2007;45:42-52.

[12] Hoshida Y, Nijman SM, Kobayashi M, Chan JA, Brunet JP, Chiang DY, et al. Integrative transcriptome analysis reveals common molecular subclasses of human hepatocellular carcinoma. Cancer research 2009;69:7385-7392.

[13] Chiang DY, Villanueva A, Hoshida Y, Peix J, Newell P, Minguez B, et al. Focal gains of VEGFA and molecular classification of hepatocellular carcinoma. Cancer research 2008;68:6779-6788.

[14] Lee JS, Chu IS, Heo J, Calvisi DF, Sun Z, Roskams T, et al. Classification and prediction of survival in hepatocellular carcinoma by gene expression profiling. Hepatology 2004;40:667-676.

[15] Guichard C, Amaddeo G, Imbeaud S, Ladeiro Y, Pelletier L, Maad IB, et al. Integrated analysis of somatic mutations and focal copy-number changes identifies key genes and pathways in hepatocellular carcinoma. Nature genetics 2012;44:694-698.

[16] Schulze K, Imbeaud S, Letouze E, Alexandrov LB, Calderaro J, Rebouissou S, et al. Exome sequencing of hepatocellular carcinomas identifies new mutational signatures and potential therapeutic targets. Nature genetics 2015;47:505-511.

[17] Totoki Y, Tatsuno K, Covington KR, Ueda H, Creighton CJ, Kato M, et al. Trans-ancestry mutational landscape of hepatocellular carcinoma genomes. Nature genetics 2014;46:1267-1273.

[18] Nault JC, Calderaro J, Di Tommaso L, Balabaud C, Zafrani ES, Bioulac-Sage P, et al. Telomerase reverse transcriptase promoter mutation is an early somatic genetic alteration in the transformation of premalignant nodules in hepatocellular carcinoma on cirrhosis. Hepatology 2014;60:1983-1992.

[19] Nault JC, Mallet M, Pilati C, Calderaro J, Bioulac-Sage P, Laurent C, et al. High frequency of telomerase reverse-transcriptase promoter somatic mutations in hepatocellular carcinoma and preneoplastic lesions. Nature communications 2013;4:2218.
[20] Ahn SM, Jang SJ, Shim JH, Kim D, Hong SM, Sung CO, et al. A genomic portrait of resectable hepatocellular carcinomas: Implications of RB1 and FGF19 aberrations for patient stratification. Hepatology 2014.
[21] Salomao M, Remotti H, Vaughan R, Siegel AB, Lefkowitch JH, Moreira RK. The steatohepatitic variant of hepatocellular carcinoma and its association with underlying steatohepatitis. Human pathology 2012;43:737-746.
[22] Shibahara J, Ando S, Sakamoto Y, Kokudo N, Fukayama M. Hepatocellular carcinoma with steatohepatitic features: a clinicopathological study of Japanese patients. Histopathology 2014;64:951-962.
[23] Mounajjed T, Chandan VS, Torbenson MS, SpringerLink (Online service). Surgical Pathology of Liver Tumors. p. IX, 477 p. 620 illus.
[24] Gao J, Aksoy BA, Dogrusoz U, Dresdner G, Gross B, Sumer SO, et al. Integrative analysis of complex cancer genomics and clinical profiles using the cBioPortal. Science signaling 2013;6:pl1.
[25] Cerami E, Gao J, Dogrusoz U, Gross BE, Sumer SO, Aksoy BA, et al. The cBio cancer genomics portal: an open platform for exploring multidimensional cancer genomics data. Cancer discovery 2012;2:401-404.
[26] Calderaro J, Labrune P, Morcrette G, Rebouissou S, Franco D, Prevot S, et al. Molecular characterization of hepatocellular adenomas developed in patients with glycogen storage disease type I. Journal of hepatology 2013;58:350-357.
[27] Huang A, Zhao X, Yang XR, Li FQ, Zhou XL, Wu K, et al. Circumventing intratumoral heterogeneity to identify potential therapeutic targets in hepatocellular carcinoma. Journal of hepatology 2017.
[28] Zhai W, Lim TK, Zhang T, Phang ST, Tiang Z, Guan P, et al. The spatial organization of intra-tumour heterogeneity and evolutionary trajectories of metastases in hepatocellular carcinoma. Nature communications 2017;8:4565.
[29] Villanueva A, Hoshida Y, Battiston C, Tovar V, Sia D, Alsinet C, et al. Combining clinical, pathology, and gene expression data to predict recurrence of hepatocellular carcinoma. Gastroenterology 2011;140:1501-1512 e1502.
[30] Rebouissou S, Franconi A, Calderaro J, Letouze E, Imbeaud S, Pilati C, et al. Genotype-phenotype correlation of CTNNB1 mutations reveals different ss-catenin activity associated with liver tumor progression. Hepatology 2016.
[31] Audard V, Grimber G, Elie C, Radenen B, Audebourg A, Letourneur F, et al. Cholestasis is a marker for hepatocellular carcinomas displaying beta-catenin mutations. The Journal of pathology 2007;212:345-352.
[32] Ueno A, Masugi Y, Yamazaki K, Komuta M, Effendi K, Tanami Y, et al. OATP1B3 expression is strongly associated with Wnt/beta-catenin signalling and represents the transporter of gadoxetic acid in hepatocellular carcinoma. Journal of hepatology 2014;61:1080-1087.
[33] Kitao A, Zen Y, Matsui O, Gabata T, Kobayashi S, Koda W, et al. Hepatocellular carcinoma: signal intensity at gadoxetic acid-enhanced MR Imaging--correlation with molecular transporters and histopathologic features. Radiology 2010;256:817-826.
[34] Anson M, Crain-Denoyelle AM, Baud V, Chereau F, Gougelet A, Terris B, et al. Oncogenic beta-catenin triggers an inflammatory response that determines the aggressiveness of hepatocellular carcinoma in mice. The Journal of clinical investigation 2012;122:586-599.
[35] Spranger S, Bao R, Gajewski TF. Melanoma-intrinsic beta-catenin signalling prevents anti-tumour immunity. Nature 2015;523:231-235.
[36] Sugino T, Kusakabe T, Hoshi N, Yamaguchi T, Kawaguchi T, Goodison S, et al. An invasion-independent pathway of blood-borne metastasis: a new murine mammary tumor model. The American journal of pathology 2002;160:1973-1980.

[37] Fang JH, Zhou HC, Zhang C, Shang LR, Zhang L, Xu J, et al. A novel vascular pattern promotes metastasis of hepatocellular carcinoma in an epithelial-mesenchymal transition-independent manner. Hepatology 2015;62:452-465.
[38] Gerald D, Chintharlapalli S, Augustin HG, Benjamin LE. Angiopoietin-2: an attractive target for improved antiangiogenic tumor therapy. Cancer research 2013;73:1649-1657.
[39] Rigamonti N, Kadioglu E, Keklikoglou I, Wyser Rmili C, Leow CC, De Palma M. Role of angiopoietin-2 in adaptive tumor resistance to VEGF signaling blockade. Cell reports 2014;8:696-706.
[40] Ando S, Shibahara J, Hayashi A, Fukayama M. beta-catenin alteration is rare in hepatocellular carcinoma with steatohepatitic features: immunohistochemical and mutational study. Virchows Archiv : an international journal of pathology 2015.
[41] Seok JY, Na DC, Woo HG, Roncalli M, Kwon SM, Yoo JE, et al. A fibrous stromal component in hepatocellular carcinoma reveals a cholangiocarcinoma-like gene expression trait and epithelial-mesenchymal transition. Hepatology 2012;55:1776-1786.
[42] Tan PS, Nakagawa S, Goossens N, Venkatesh A, Huang T, Ward SC, et al. Clinicopathological indices to predict hepatocellular carcinoma molecular classification. Liver international : official journal of the International Association for the Study of the Liver 2015.

Figure legends

Figure 1. (A) Gross, microscopic and immunohistochemical features associated with *CTNNB1* mutations. (B) Gross appearance of a *CTNNB1* mutated tumour: the tumour has an intact capsule and a green color due to bile production. (C) Microscopic features of a *CTNNB1* mutated HCC: microtrabecular and pseudoglandular architectural pattern with numerous bile plugs within the lumens of the pseudoglands (black arrows) (#CHC1715T). (D) Nuclear β-catenin staining (left panel, #CHC1715T) with strong GS expression (right panel, #CHC1715T). (E) Gene expression profiling of *CTNNB1* mutated tumours: maintenance of markers of hepatocellular differentiation and function, low cell proliferation, dysregulation in bile salts transporters expression with up-regulation of transporters involved in canalicular bile salts efflux and down-regulation of transporters responsible for bile salts efflux into blood flow, low IL6/JAK/STAT pathway activation and upregulation of Wnt/β-catenin pathway targets (*CTNNB1* mutated cases n=35; *CTNNB1* non-mutated cases, n=149). (F) Schematic representation of a *CTNNB1* mutated neoplastic cell: the dysregulation of bile salts transporters (upregulation=red, down regulation= green) leads to bile salts uptake from the blood flow and excretion into the canaliculi (pseudogland lumen). HES=Hematein-Eosin-Saffron, Expres= expression, T=tumour, NT=non-tumour. Comparison between qualitative and quantitative data was performed using Chi-square and Fisher exact tests and Mann-Whitney U and Kruskall-Wallis tests, respectively. Monte-Carlo method was used to adjust the P value for multiple tests.

Figure 2. (A) Gross, microscopic and immunohistochemical features associated with *TP53* mutations. (B) Micrographs of compact (left panel) and macrotrabecular (right panel) architectural patterns. (C) Micrographs of pleomorphic (black arrow) and multinucleated (white arrow) cells (left panel, #CHC1754T), and sarcomatous changes characterized by elongated neoplastic cells embedded in a fibrous stroma (black arrow, right panel, #CHC1182T). (D) RT-PCR expriments showed increased cell profileration

and activation of epithelial-to-mesenchymal transition and angiogenesis (*TP53* mutated HCCs n=37, *TP53* non-mutated HCCs n=149). (E) Heat-map graphical representation of the main pathological and immunohistochemical features linked to *CTNNB1* and *TP53* mutational status (series with available immunohistochemistry, n=219). HES: Hematein-Eosin-Saffron, Mut=mutation, T=tumour, NT=non-tumour. Comparison between qualitative and quantitative data was performed using Chi-square and Fisher exact tests and Mann-Whitney U and Kruskall-Wallis tests, respectively. Monte-Carlo method was used to adjust the P value for multiple tests.

Figure 3. (A) Low magnification of a macrotrabecular-massive HCC, with a vascular invasion (VI) and a satellite nodule (SN) located outside the main tumour (T) (#CHC1754T). (B) Identification of a predominant macrotrabecular pattern in this low-power microcopic field (#CHC1754T). (C) Thick macrotrabeculae coated by endothelial cells and surrounded by vascular spaces (#CHC1754T). (D) Trabeculae appearing as tumour clusters when observed in cross sections (#CHC1754T). (E) Associations between macrotrabecular-massive HCC subtype and clinical, pathological and molecular features in both cohorts (for RT-PCR experiments of InsermU1162 cohort MTM-HCC n=12, Non MTM-HCC n=174; for RNA sequencing experiments of TCGA cohort MTM-HCC n=61, Non MTM-HCC n=292). (F) Association of macrotrabecular-massive HCC with early relapse and shorter disease-specific survival. HES=Hematein-Eosin-Saffron, T=tumour, NT=non-tumour, Mut=mutation, Expres=expression, Amp=amplification, EFS=Event-free survival, na=not available. Comparison between qualitative and quantitative data was performed using Chi-square and Fisher exact tests and Mann-Whitney U and Kruskall-Wallis tests, respectively. Monte-Carlo method was used to adjust the P value for multiple tests. **ANGPT2* expression data from the TCGA cohort was compared using the z-scores provided on the TCGA webportal.

Figure 4. (A) A scirrhous HCC with dense, hyalin stroma surrounding clusters of neoplastic cells (#CHC1198T). (B) Schirrhous HCC with CK19 expression (#CHC1182T). (C) Associations between the scirrhous subtype of HCC and molecular and immunohistochemical features. (D) Upregulation of progenitor/cancer stem cell genes and activation of epithelial-to-mesenchymal transition (Scirrhous HCCs n=12, non-scirrhous HCCs n=174). (E) A case of steatohepatitic HCC with cell ballooning, steatosis, Mallory-Denk bodies and inflammation (#CHC1712T). (F) Associations between the steatohepatitic subtype of HCC and pathological and molecular features. HES: Hematein-Eosin-Saffron, Mut.=mutation, Expres.=expression, T=tumour, NT=non-tumour. Comparison between qualitative and quantitative data was performed using Chi-square and Fisher exact tests and Mann-Whitney U and Kruskall-Wallis tests, respectively. Monte-Carlo method was used to adjust the P value for multiple tests.

Figure 5. Integration of clinical, pathological and molecular features into HCC molecular classification. Mut=mutation, ampl=amplification. Comparison between qualitative data was performed using Chi-square and Fisher exact test. Monte-Carlo method was used to adjust the P value for multiple tests.

Table 1. Clinical, phenotypical and molecular features of the series.

Variables		Available data (n)	n (%)
Age	>60 years	343	234 (68%)
Gender	Male/Female	343	293 (85%)/50 (15%)
Etiology	Alcohol/HBV/HCV/Hemochromatosis	337	138 (41%)/58 (17%)/61 (18%)/28 (8%)
	MS/Undetermined	335	58 (17%)/ 39 (8%)
BCLC	0/A/B/C	343	12 (3%)/220 (64%)/57 (17%)/54 (16%)
Preoperative serum Alpha-Foeto Protein	>100 ng/ml	278	76 (28%)
Histological and gross features of the tumors	Tumor size>50mm	343	208 (61%)
	Intact tumour capsule	342	38 (11%)
	Satellite Nodules	343	157 (46%)
	Macrovascular invasion, Microvascular invasion	343	56 (18%)/205 (60%)
	Edmonson grade: I-II/III-IV	343	147 (43%)/196 (57%)
	Architectural pattern: Microtrabecular/ Macrotrabecular/Pseudoglandular/Compact	343	252 (73%)/180 (52%)/182 (53%)/156 (45%)
	Tumoral cholestasis/ Clear cells	343	86 (25%)/105 (31%)
	Pleomorphic cells/Multinucleated cells	343	21 (6%)/76 (22%)
	Tumoral steatosis	343	98 (29%)
	Sarcomatous changes/Hyaline bodies	343	39 (11%)/55 (16%)
	Macrotrabecular-massive/Steatohepatitic subtype	343	36 (10%)/20 (6%)
	Scirrhous/Lymphoepithelioma-like subtype	343	18 (5%)/6 (2%)
Non tumor liver fibrosis	METAVIR F0-F1/F2-F3/F4	343	130 (38%)/113 (33%)/99 (29%)
Immunohistochemical phenotype of the tumors	β-catenin nuclear expression/GS strong and diffuse staining	218	78 (36%)/84 (39%)
	CK19/EPCAM expression	219/218	16 (7%)/30 (14%)
	CRP/ARID1A expression	214/216	118 (55%)/153 (71%)
	Phospho-S6 expression (mean % of stained cells, range)	211	32% (0-100)
	Phospho-ERK expression	203	21 (10%)
Gene alterations	*TERT promoter*	322	208 (65%)
	CTNNB1	332	130 (40%)
	TP53	341	72 (21%)
	ALB	170	27 (16%)
	ARID1A	313	45 (14%)
	AXIN1	322	34 (11%)
	APOB	171	18 (11%)
	ARID2	313	23 (7%)
	NFE2L2	308	19 (6%)
	TSC1/TSC2	239	15 (6%)
	ATM	238	15 (6%)
	RPS6KA3	311	16 (5%)
	CDKN2A	129	7 (5%)
	ACVR2A	129	6 (5%)

	FGF19 amplifications	129	6 (5%)
Trancriptomic subgroups	G1/G2/ G3/ G4/G5/G6	265	13 (5%)/15 (6%)/52 (20%)/91 (34%)/61 (23%)/32 (12%)

Table 2. Analysis of clinical, biological and histological features for disease-specific survival (InsermU1162 Cohort, n=278, only features with more than 10% infrequency were selected) (OR= Odds Ratio, CI=Confidence Interval). Statistical analysis was performed using univariate and multivariate Cox proportional hazards regression models (Wald test).

	Early reccurrence				**Disease-specific survival**			
	Univariate analysis		**Multivariate analysis**		**Univariate analysis**		**Multivariate analysis**	
	OR (CI 95%)	**p value**	**OR (CI 95%)**	**p value**	**OR (CI 95%)**	**p value**	**OR (CI 95%)**	**p value**
Clinical and biological features								
Age>60 years	1.06 (0.72-1.57)	0.71			0.90 (0.52-1.57)	0.71		
Male sex	1.23 (0.71-2.11)	0.45			1.42 (0.61-3.32)	0.42		
BCLC stage B-C*	**2.38 (1.64-3.42)**	**<0.001**			**3.25 (1.89-5.58)**	**<0.001**		
Alcohol	0.94 (0.65-1.37)	0.77			1.20 (0.71-2.05)	0.49		
HCV infection	1.32 (0.86-2.04)	0.20			0.91 (0.46-1.81)	0.79		
HBV infection	1.15 (0.72-1.85)	0.56			1.45 (0.76-2.75)	0.26		
Metabolic syndrome	0.69 (0.38-1.26)	0.23			0.65 (0.26-1.64)	0.36		
AFP serum level >100ng/ml	1.43 (0.95-2.18)	0.09			**2.6 (1.47-4.61)**	**0.001**	1.44 (0.77-2.67)	0.25
Pathological features								
Tumor size>50mm	1.42 (0.97-2.08)	0.08			**2.53 (1.30-4.91)**	**0.004**	1.19 (0.56-2.52)	0.65
Intact tumour capsule	0.57 (0.27-1.23)	0.15			0.52 (0.16-1.67)	0.26		
Satellite Nodules	**3.40 (2.31-5.02)**	**<0.001**	**2.02 (1.28-3.18)**	**0.002**	**4.60 (2.47-8.60)**	**<0.001**	1.68 (0.77)-3.67)	0.19
Macrovascular invasion*	**3.54 (2.39-5.26)**	**<0.001**	**1.82 (1.17-2.86)**	**0.008**	**6.00 (3.51-10.28)**	**<0.001**	**2.80 (1.47-5.35)**	**0.002**
Microvascular invasion	**2.85 (1.88-4.31)**	**<0.001**	1.60 (0.97-2.62)	0.06	**8.24 (3.28-20.7)**	**<0.001**	**3.24 (1.04-10.06)**	**0.04**
Edmonson grade III-IV	**1.57 (1.08-2.27)**	**0.004**	1.29 (0.86-1.93)	0.21	**3.13 (1.65-5.94)**	**<0.001**	1.59 (0.79-3.20)	0.19
Microtrabecular pattern	0.99 (0.66-1.49)	0.63			0.65 (0.38-1.15)	0.14		
Macrotrabecular pattern*	**1.79 (1.23-2.62)**	**0.002**			**3.29 (1.73-6.25)**	**<0.001**		
Compact pattern	0.88 (0.61-1.29)	0.54			0.88 (0.51-1.53)	0.66		
Pseudoglandular	0.82 (0.57-1.19)	0.30			0.74 (0.43-1.26)	0.26		

pattern								
Inflammatory infiltrates	**0.64 (0.42-0.99)**	**0.02**	0.65 (0.41-1.02)	0.06	0.57 (0.29-1.11)	0.09		
Cholestasis	1.19 (0.79-1.79)	0.70			0.84 (0.44-1.61)	0.61		
Clear cells	0.80 (0.53-1.21)	0.42			0.97 (0.53-1.76)	0.92		
Multinucleated cells	0.87 (0.54-1.39)	0.47			1.49 (0.82-2.71)	0.18		
Tumour steatosis	0.78 (0.52-1.18)	0.16			0.71 (0.47-1.07)	0.09		
Sarcomatous changes	0.78 (0.43-1.43)	0.48			0.80 (0.32-2.01)	0.63		
Hyaline bodies	0.94 (0.59-1.50)	0.68			0.88 (0.43-1.81)	0.73		
Macrotrabecular-massive subtype*	**2.88 (1.71-4.83)**	**<0.001**	**1.70 (0.99-2.91)**	**0.05**	**5.68 (3.07-10.47)**	**<0.001**	**2.19 (1.06-4.50)**	**0.03**
METAVIR F0-F1	0.94 (0.65-1.36)	0.66			0.79 (0.45-1.40)	0.42		
METAVIR F2-F3	0.90 (0.61-1.32)	0.48			0.88 (0.50-1.57)	0.67		
METAVIR F4	1.21 (0.82-1.79)	0.21			1.46 (0.83-2.55)	0.18		

**For collinear variables (BCLC B-C and macrovascular invasion; macrotrabecular histological pattern and macrotrabecular-massive subtype), a bivariate analysis was performed prior to the multivariate analysis. The variable with the highest OR was further included in the multivariate analysis.*

Figure 1

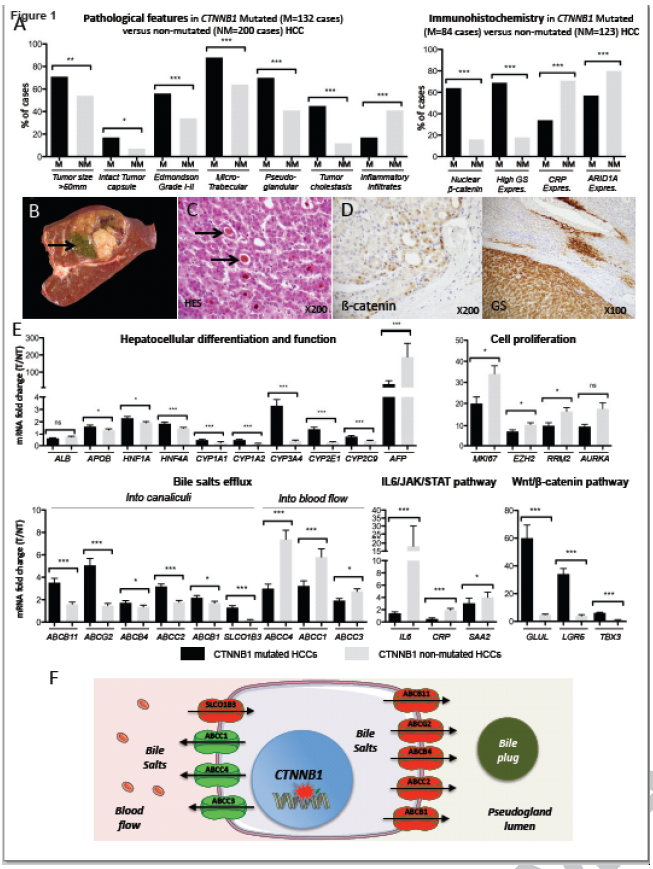

Figure 2

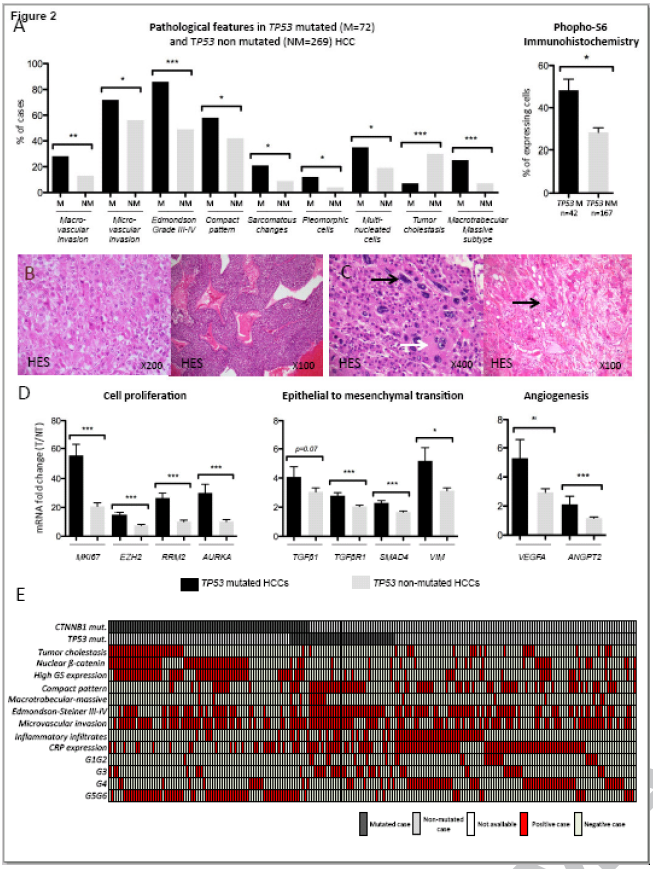

Figure 3

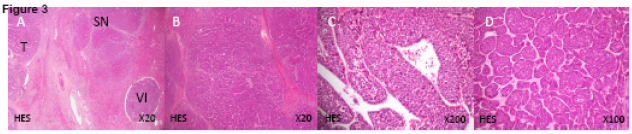

E

	InsermU1162 Cohort			TCGA Cohort		
Variables	Macrotrabecular-massive HCC (MTM-HCC)	Non macrotrabecular-massive HCC (Non MTM-HCC)	p value	Macrotrabecular-massive HCC (MTM-HCC)	Non macrotrabecular-massive HCC (Non MTM-HCC)	p value
High AFP (>100 ng/ml)	53% (32/54)	25% (64/254)	0.02	54% (21/39)	27% (63/233)	0.001
HBV infection	35% (12/34)	15% (46/305)	0.01	na	na	na
Satellite nodules	78% (28/36)	42% (129/307)	<2.001	na	na	na
Macrovascular invasion	53% (18/34)	12% (36/307)	<2.001	16% (6/40)	3% (9/255)	0.002
Microvascular invasion	94% (34/36)	56% (171/307)	<2.001	55% (26/48)	30% (77/255)	0.003
CK19 expression	23% (4/17)	6% (12/202)	0.02	na	na	na
G3 subgroup	54% (12/22)	16% (40/243)	<2.001	na	na	na
TP53 mutations	53% (18/34)	18% (54/305)	<2.001	56% (34/61)	26% (79/297)	<0.001
FGF19 amplifications	33% (2/6)	3% (4/123)	0.02	15% (9/61)	5% (14/297)	0.007
ATM mutations	20% (4/20)	5% (11/218)	0.03	2% (1/61)	3% (9/297)	1
ANGPT2 expression (mean, SEM)	5.18 (0.83)	3.33 (0.35)	0.034	0.55*	-2.06*	<0.001
VEGFA expression (mean, SEM)	1.57 (0.26)	1.36 (0.14)	0.07	na	na	na

F

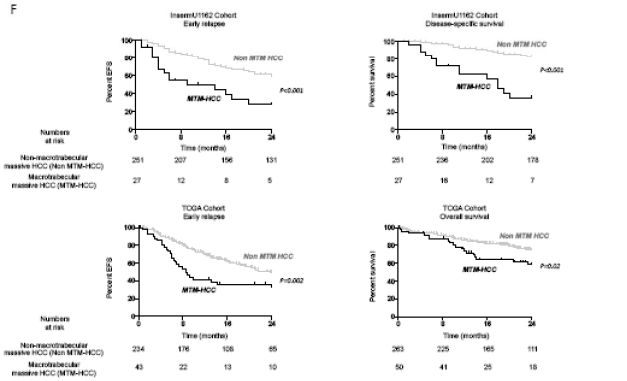

Figure 4

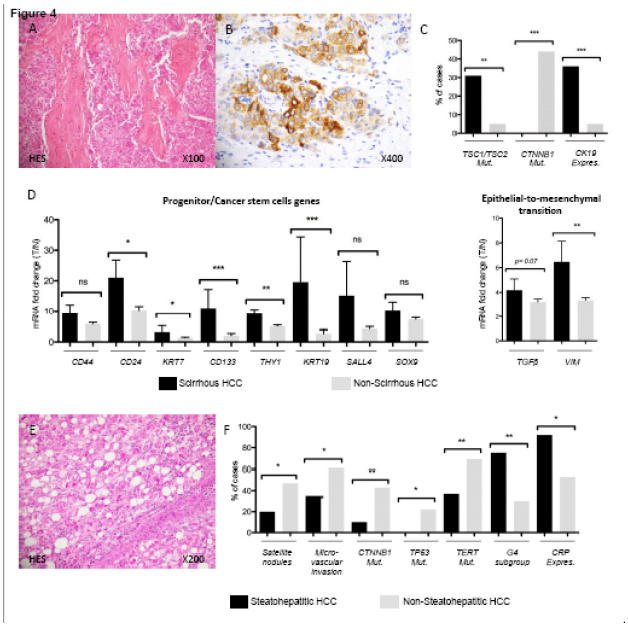

Figure 5

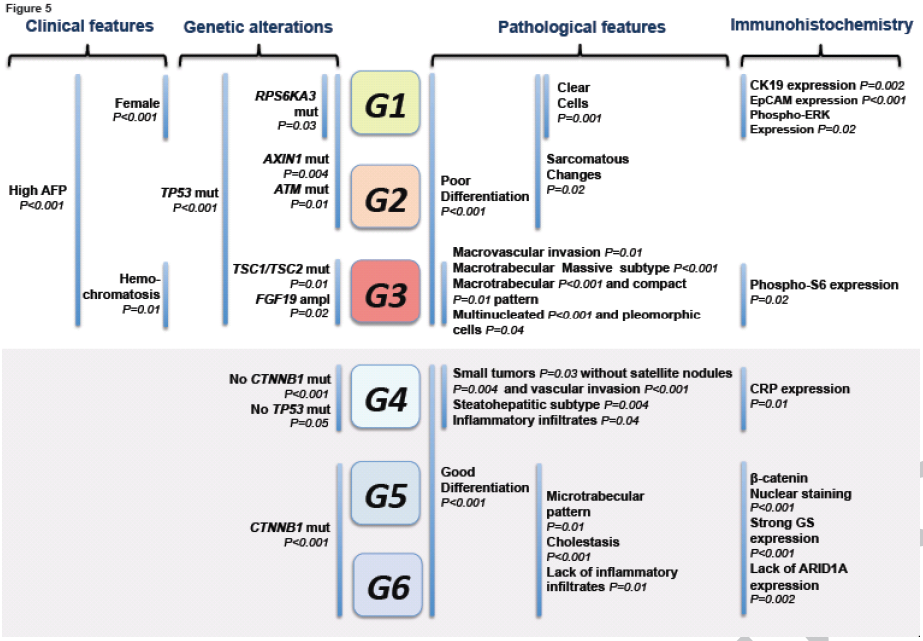

-*CTNNB1* and *TP53* mutations are mutually exclusive and define two major groups of HCC characterized by distinct phenotypes.

-Histological subtypes recognized by the World Health Organisation of Tumours are strongly related to particular oncogenic pathways and molecular alterations.

-We have identified a novel HCC histological subtype, designated as "macrotrabecular-massive" (MTM-HCC), associated with a poor clinical outcome, *TP53* mutations, *FGF19* amplifications and vascular invasion.

-The close relationship between HCC phenotype and its underlying molecular alterations may help in translating our knowledge of HCC biology into clinical practice.